

# Comparative Theoretical Analysis of Entangled Quantum States for Enhanced Sensing Applications

Kelvin Mpofu<sup>1</sup> and Patience Mthunzi-Kufa<sup>2</sup>

<sup>1</sup>Biophotonics, Photonic Centre, Manufacturing, Council of Scientific and Industrial Research (CSIR), Pretoria, South Africa

<sup>2</sup>School of Interdisciplinary Research and Graduate Studies (UNESCO), College of Graduate Studies, University of South Africa, Preller Street, Muckleneuk Ridge, Pretoria, South Africa

E-mail: [kmpofu@csir.co.za](mailto:kmpofu@csir.co.za)

**Abstract.** Quantum metrology offers a route to enhance precision measurements by exploiting non-classical states of light. In this paper, we present a comparative theoretical analysis of phase sensitivity across several entangled quantum states, NOON, M&M, Twisted NOON, GHZ, Entangled Coherent States (ECS), and BAT states, under ideal conditions. Our findings reveal that Twisted NOON states achieve the highest enhancement in precision, surpassing even the Heisenberg limit due to orbital angular momentum contributions. The results highlight the value of tailoring quantum states to specific metrological tasks and provide a foundation for future experimental realizations in quantum sensing.

## 1 Introduction

In an era where precision underpins progress, metrology, the science of measurement, plays a foundational role across scientific and technological domains [1]. From calibrating atomic clocks to aligning satellite systems and enhancing diagnostic imaging, precise measurement systems are indispensable [2, 3]. Classical metrology, particularly optical interferometry, has long served as the gold standard in achieving high-precision measurements [4]. However, its capabilities are ultimately bounded by the Standard Quantum Limit (SQL), a fundamental sensitivity ceiling imposed by quantum noise associated with independent particles or photons [5]. Quantum metrology [6] seeks to transcend this boundary by harnessing non-classical resources, most notably quantum entanglement and squeezing. These uniquely quantum phenomena enable phase sensitivities that scale more favorably with resource number, often reaching or surpassing the Heisenberg Limit (HL), where phase uncertainty scales as  $\Delta\phi \sim 1/N$  as opposed to the SQL which scales as  $\Delta\phi \sim 1/\sqrt{N}$  [7]. The realization of this quantum advantage has profound implications for next-generation sensing, imaging, and navigation systems [7].

Numerous experimental efforts have demonstrated the feasibility of preparing the quantum states analyzed in this work. Coherent states, the cornerstone of classical optics, are readily produced using stable laser sources and are foundational in all quantum optics laboratories. NOON states have been experimentally realized in photonic platforms, with successful demonstrations up to five-photon NOON states using spontaneous parametric down-conversion and beam splitters, as reported by Afek et al. [8]. The experimental preparation of M&M states was demonstrated for M=3 by Smith [9]. GHZ states, another maximally entangled resource, have been extensively realized across diverse platforms including photons, trapped ions, and superconducting qubits [10, 11]. Twisted NOON states, which embed orbital angular momentum (OAM) into entangled photons, have been generated using spatial light modulators and tailored optical elements, with experiments by Yang et al. [12]. Entangled Coherent States (ECS) have been synthesized in cavity-QED and trapped-ion platforms using techniques [13]. Lastly,

BAT states, which resemble symmetric ECS but are phase-insensitive, have not always been labeled explicitly in experimental work but have analogues in delocalized single-photon interference experiments. Together, these experimental demonstrations provide strong support for the physical realizability of the quantum resources assessed in this comparative study.

Among the most promising candidates for quantum-enhanced metrology are entangled states of light. These include NOON states [7], GHZ states [14], ECS [15], and more recent variants such as Twisted NOON [12] and M&M states. Each of these states offers different trade-offs between sensitivity, robustness, and experimental feasibility. Yet, a unified theoretical comparison of their phase precision performance under ideal conditions remains essential for guiding experimental design and deployment in real-world sensing platforms.

This paper presents a comparative theoretical analysis of key entangled quantum states in the context of phase estimation, arguably the most fundamental task in optical quantum metrology. Other works do not put all the quantum states in one place for comparison. This work provides an extensive and more universal comparison of entangled states for sensing. Using analytical and numerical tools, we evaluate their performance based on Fisher Information and the Cramér-Rao bound. By doing so, we identify the quantum states best suited for achieving precision beyond the SQL and highlight the physical principles that enable their superior performance. The results serve as a roadmap for the rational design of entangled-state-based quantum sensors and provide insight into the fundamental limits of measurement precision.

## 2 Quantum sensing model

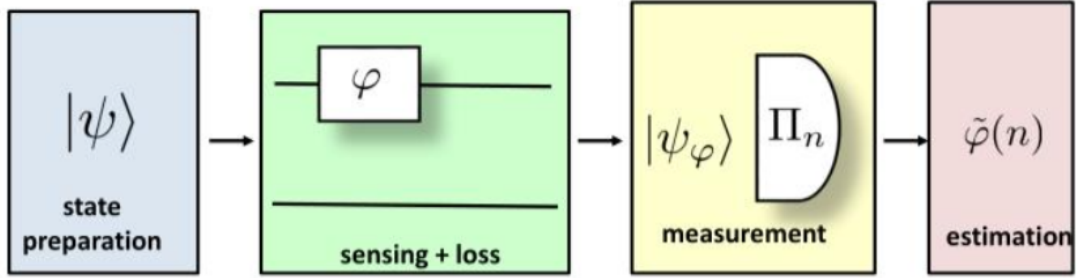


Figure 1: Schematic representation of a quantum metrology protocol. The process consists of four main stages: state preparation, sensing with loss, measurement, and estimation [16].

Description of the Protocol shown in Figure 1:

- **State Preparation**  $|\psi\rangle$ : A quantum state is prepared with the goal of enhancing sensitivity to an unknown parameter  $\varphi$ . Commonly used probe states include NOON, GHZ, M&M, Entangled Coherent States (ECS), and BAT states. These states typically exhibit quantum correlations or entanglement that are leveraged for sub-classical precision.
- **Sensing + Loss** ( $\varphi$ ): The quantum state undergoes evolution under the parameter of interest, typically a phase shift  $\varphi$ . This is modeled as a unitary transformation  $U(\varphi) = e^{i\varphi\hat{G}}$ , where  $\hat{G}$  is the generator (often the photon number operator). Simultaneously, photon loss is introduced via noise channels such as amplitude damping or beam-splitter models, impacting the fidelity and precision of the state.
- **Measurement** ( $|\psi_\varphi\rangle, \Pi_n$ ): After evolution, the state  $|\psi_\varphi\rangle$  is measured using a suitable set of positive operator-valued measures (POVMs)  $\{\Pi_n\}$ . This results in a distribution of outcomes  $n$  that are dependent on  $\varphi$ . Measurement strategies (e.g., parity, photon counting, homodyne) influence the achievable sensitivity.
- **Estimation** ( $\tilde{\varphi}(n)$ ): An estimator  $\tilde{\varphi}(n)$  is applied to infer the parameter  $\varphi$  from the outcomes. The estimation performance is bounded by the quantum Cramér-Rao inequality:

$$\Delta\varphi \geq \frac{1}{\sqrt{F_Q[\rho_\varphi]}}$$

where  $F_Q[\rho_\varphi]$  is the quantum Fisher information of the evolved (and possibly mixed) state. Different probe states offer different precision scalings, from the SQL to the Heisenberg limit, depending on their quantum resources and robustness to loss.

### 3 Quantum states

This study investigates the theoretical phase sensitivity of various entangled quantum states in idealized interferometric metrology scenarios. The analysis is based on well-established tools in quantum estimation theory, namely the quantum Fisher information (QFI) and the Cramér-Rao bound, which provide lower limits on the precision of parameter estimation. In this study, we analyzed a variety of quantum states commonly proposed for enhanced phase estimation in optical interferometry. Each state represents a different quantum resource configuration with distinct precision scaling properties. The states are defined as follows:

- **NOON State:**

$$|\psi_{\text{NOON}}\rangle = \frac{1}{\sqrt{2}} (|N\rangle_a |0\rangle_b + |0\rangle_a |N\rangle_b).$$

Where  $|N\rangle$ : Fock state with  $N$  photons (or particles) in a given mode.  $a, b$  are optical modes or interferometer arms (e.g., input/output ports of a Mach-Zehnder interferometer). This maximally path-entangled state achieves Heisenberg-limited phase sensitivity but is highly susceptible to photon loss.

- **M&M State:**

$$|\psi_{\text{M\&M}}\rangle = \frac{1}{\sqrt{2}} (|M\rangle_a |m\rangle_b + |m\rangle_a |M\rangle_b), \quad \text{with } M - m = N$$

A generalization of the NOON state with tunable imbalance, offering improved robustness at the cost of reduced entanglement.

- **Twisted NOON State:**

$$|\psi_{\text{Twisted}}\rangle = \frac{1}{\sqrt{2}} (|N, +\ell\rangle_a |0\rangle_b + |0\rangle_a |N, -\ell\rangle_b)$$

This state incorporates orbital angular momentum  $\ell$ , which improves sensitivity to angular displacement and offers enhanced phase precision scaling as  $\Delta\phi \sim 1/(\ell N)$ .

- **GHZ State:**

$$|\psi_{\text{GHZ}}\rangle = \frac{1}{\sqrt{2}} (|0\rangle^{\otimes N} + |1\rangle^{\otimes N})$$

A multipartite entangled state analogous to the NOON state for qubits, achieving Heisenberg scaling in spin-based or atomic systems.

- **Entangled Coherent State (ECS):**

$$|\psi_{\text{ECS}}\rangle = \mathcal{N}_\alpha (|\alpha\rangle_a |0\rangle_b + |0\rangle_a |\alpha\rangle_b)$$

where  $\mathcal{N}_\alpha = [2(1 + e^{-|\alpha|^2})]^{-1/2}$  is the normalization constant. ECSs are optical analogs of cat states and offer sub-Heisenberg scaling under ideal conditions.

- **BAT State (Balanced Amplified Two-mode state):**

$$|\psi_{\text{BAT}}\rangle = \frac{1}{\sqrt{2}} (|\alpha\rangle_a |0\rangle_b + |0\rangle_a |\alpha\rangle_b)$$

A simplified state with moderate entanglement and practical stability, suitable for experimental implementations with limited resources.

- **Coherent State (Classical Benchmark):**

$$|\psi_{\text{coh}}\rangle = |\alpha\rangle_a |\beta\rangle_b$$

Here,  $|\alpha\rangle$  and  $|\beta\rangle$  are coherent states in modes  $a$  and  $b$ , respectively. These states follow classical statistics and are limited by the standard quantum limit  $\Delta\phi \sim 1/\sqrt{N}$ .

### Phase Estimation Framework

The phase estimation process is modeled within the configuration shown in Fig. . Each quantum state is subjected to a unitary phase shift  $U(\phi) = \exp(i\phi\hat{n})$  on one arm of the interferometer, where  $\hat{n}$  is the photon number operator. For each quantum state, we compute the quantum Fisher information  $\mathcal{F}_Q$ , which quantifies the sensitivity of the state to small changes in the phase  $\phi$ . The ultimate phase precision limit is then given by the quantum Cramér-Rao bound:

$$\Delta\phi \geq \frac{1}{\sqrt{\mathcal{F}_Q}}. \quad (1)$$

This provides a lower bound on the standard deviation of any unbiased phase estimator.

## 4 Quantum Cramér-Rao Bound and Fisher Information

### Quantum Cramér-Rao Inequality

$$\Delta^2\tilde{\phi} \geq \frac{1}{F_Q[\rho_\varphi]} \quad (2)$$

### Quantum Fisher Information Definitions

For a general quantum state  $\rho_\varphi$ , the QFI is given by:

$$F_Q[\rho_\varphi] = \text{Tr}(\rho_\varphi A_\varphi^2) \quad (3)$$

where  $A_\varphi$  is the symmetric logarithmic derivative (SLD) defined via:

$$\frac{d\rho_\varphi}{d\varphi} = \frac{1}{2}(\rho_\varphi A_\varphi + A_\varphi \rho_\varphi) \quad (4)$$

### For Pure States

If  $\rho_\varphi = |\psi_\varphi\rangle\langle\psi_\varphi|$ , then the QFI simplifies to:

$$F_Q[|\psi_\varphi\rangle] = 4 \left( \left| \langle \dot{\psi}_\varphi | \dot{\psi}_\varphi \rangle \right| - \left| \langle \psi_\varphi | \dot{\psi}_\varphi \rangle \right|^2 \right) \quad (5)$$

where:

$$|\dot{\psi}_\varphi\rangle = \frac{d}{d\varphi} |\psi_\varphi\rangle \quad (6)$$

### For Mixed States

The QFI for a mixed state  $\rho_\varphi$  can be calculated by minimizing the QFI over all purifications  $|\Psi_\varphi\rangle$  such that:

$$\rho_\varphi = \text{Tr}_E (|\Psi_\varphi\rangle\langle\Psi_\varphi|) \quad (7)$$

$$F_Q[\rho_\varphi] = \min_{|\Psi_\varphi\rangle} F[|\Psi_\varphi\rangle] \quad (8)$$

## 5 Results

Figures 2 and 3 illustrate the theoretical phase precision performance of the various entangled states under both ideal and lossy interferometric conditions. The performance metric used is the quantum Fisher information (QFI), which directly determines the minimum achievable phase uncertainty via the quantum Cramér-Rao bound. This work only considered the ideal cases, with the lossy case being considered for future work. As shown in Figure 2, the NOON, GHZ, and M&M (with  $M - m = N$ ) states achieve Heisenberg-limited scaling, with QFI scaling quadratically with photon number ( $F_Q \propto N^2$ ). Among these, the Twisted NOON state outperforms all others, benefiting from an additional factor of orbital angular momentum  $\ell$ , yielding a scaling of  $\Delta\phi \sim 1/(\ell N)$ . Both ECS and BAT states display sub-Heisenberg scaling under ideal conditions. However, their QFI curves remain smooth and stable, suggesting ease of generation and favorable error tolerance in practical setups. The coherent state benchmark, following the SQL ( $\Delta\phi \sim 1/\sqrt{N}$ ), is clearly outperformed by all quantum-enhanced states in the ideal case.

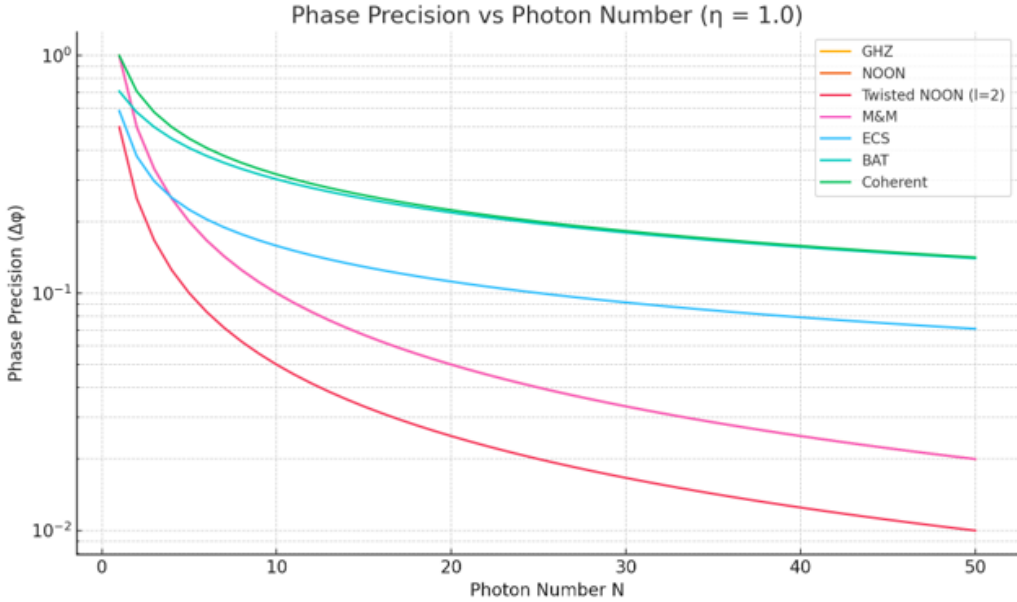


Figure 2: Phase estimation precision  $\Delta\varphi$  as a function of photon number  $N$  under ideal lossless conditions ( $\eta = 1.0$ ), comparing several quantum states including NOON, M&M (with  $M - m = N$ ), Twisted NOON ( $\ell = 2$ ), entangled coherent states (ECS), BAT states, and coherent states. The M&M configuration used here satisfies the condition  $M - m = N$ , aligning its scaling with the Heisenberg limit.

#### Quantum-to-Coherent Precision Ratio Analysis

Figure 3 presents the quantum-to-coherent phase precision ratio (which can be interpreted as an enhancement factor in the precision of the quantum state over the coherent ), defined as  $\Delta\varphi_{\text{quantum}}/\Delta\varphi_{\text{coherent}}$ , plotted as a function of photon number  $N$  under ideal (lossless) conditions ( $\eta = 1.0$ ). This ratio quantifies the enhancement in phase estimation achievable by various quantum states compared to classical coherent states. A value less than 1 indicates a quantum advantage. As expected, the NOON and GHZ states (orange and gold curves) exhibit the most substantial improvement, adhering closely to Heisenberg-limited scaling. The twisted NOON states with orbital angular momentum  $\ell = 2$  (red) further outperform standard NOON states due to their increased phase sensitivity from the additional angular degree of freedom. M&M states (pink), configured such that  $M - m = N$ , demonstrate a steady improvement with photon number, eventually exceeding the classical limit. In contrast, Entangled Coherent States (ECS, cyan) and BAT states (teal) yield precision ratios slightly below 1 across the entire range of  $N$ , indicating modest yet consistent quantum enhancements. These results collectively underscore the importance of state structure in optimizing quantum sensing protocols, especially when balancing sensitivity and scalability.

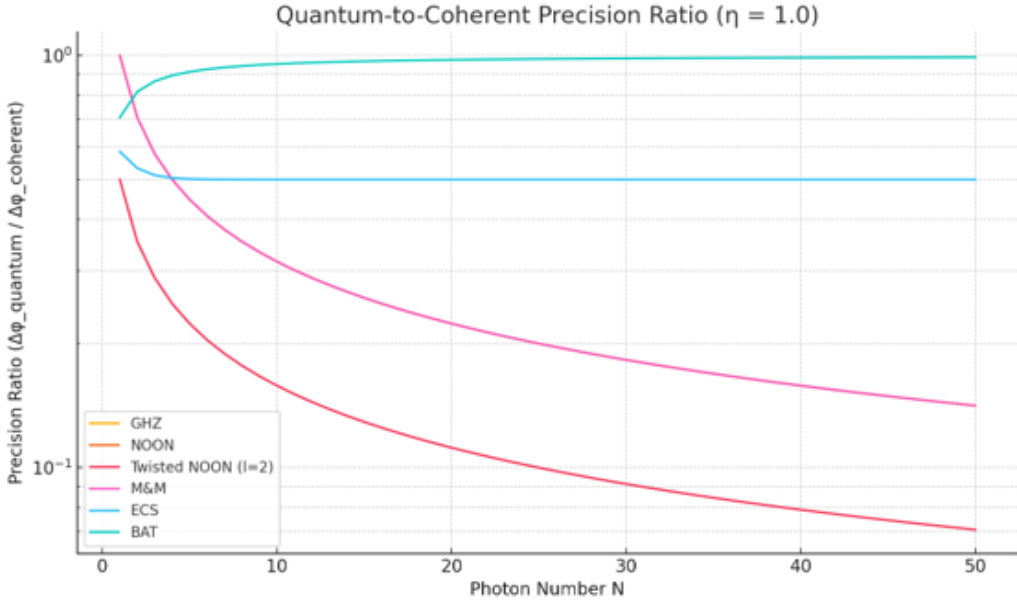


Figure 3: Quantum-to-coherent phase precision ratio as a function of photon number  $N$  in the ideal lossless case ( $\eta = 1.0$ ). The plot shows  $\Delta\varphi_{\text{quantum}}/\Delta\varphi_{\text{coherent}}$  for several quantum states including GHZ, NOON, Twisted NOON ( $\ell = 2$ ), M&M, ECS, and BAT states. Values below 1 indicate improved precision over classical coherent states. Twisted NOON and NOON states display the greatest enhancement in precision with increasing  $N$ , while ECS and BAT provide modest yet consistent improvements. The GHZ is overlapping with the NOON so it is not missing in the plot.

## 6 Conclusion

In this study, we conducted a comprehensive theoretical comparison of phase sensitivity across several entangled quantum states relevant to quantum metrology. Specifically, we analyzed NOON, GHZ, M&M, Twisted NOON, ECS, and BAT states under ideal ( $\eta = 1$ ) conditions using the QFI framework and the QCRB formalism. Our results confirm that NOON, GHZ, and M&M states (with  $M - m = N$ ) achieve Heisenberg-limited scaling, with phase precision following  $\Delta\phi \sim 1/N$ , highlighting their theoretical optimality under lossless conditions. Among these, the Twisted NOON states exhibited the highest precision, scaling as  $\Delta\phi \sim 1/(\ell N)$ , due to their incorporation of orbital angular momentum  $\ell$ , which introduces an additional degree of phase sensitivity.

By contrast, while ECS and BAT states do not achieve Heisenberg scaling, they offer enhanced robustness and practicality. Their performance remains competitive in the presence of imperfections or anticipated loss, making them favorable candidates for real-world implementations where decoherence and photon loss are non-negligible. Coherent states, used as a classical benchmark, followed the SQL  $\Delta\phi \sim 1/\sqrt{N}$ , serving as a baseline to quantify the quantum enhancement achieved. To contextualize these findings, we also introduced a Quantum-to-Coherent Precision Ratio metric, which emphasizes the relative gain over classical strategies. Twisted NOON and M&M states exhibited the most significant quantum enhancement over the full photon-number range.

The insights presented here provide a roadmap for tailoring quantum resources to specific sensing regimes. Future work will involve extending this analysis to lossy interferometric scenarios ( $\eta < 1$ ), where the relative robustness of each state can be fully evaluated. Additionally, experimental efforts can focus on hybrid entangled states, integrating benefits of both path-entanglement and coherent superpositions, possibly achieving both robustness and enhanced precision. With increasing access to photonic quantum hardware, this theoretical foundation contributes to the ongoing translation of quantum-enhanced sensing concepts into practical technologies.

## References

[1] S. Yadav, S. Rab, and M. Wan, “Metrology and sustainability in industry 6.0: Navigating a new paradigm,” in *Handbook of quality system, accreditation and conformity assessment*. Springer, 2024, pp. 855–885.

[2] D. K. Aswal, S. Yadav, T. Takatsuji, P. Rachakonda, and H. Kumar, *Handbook of Metrology and Applications*. Springer Nature, 2023.

[3] K. Kassem, “Interferometric intensity correlation: from sensing to imaging,” Ph.D. dissertation, University of Glasgow, 2024.

[4] G. Huang, C. Cui, X. Lei, Q. Li, S. Yan, X. Li, and G. Wang, “A review of optical interferometry for high-precision length measurement,” *Micromachines*, vol. 16, no. 1, p. 6, 2024.

[5] V. Giovannetti, S. Lloyd, and L. Maccone, “Quantum-enhanced measurements: beating the standard quantum limit,” *Science*, vol. 306, no. 5700, pp. 1330–1336, 2004.

[6] M. A. Taylor and W. P. Bowen, “Quantum metrology and its application in biology,” *Physics Reports*, vol. 615, pp. 1–59, 2016.

[7] J. P. Dowling, “Quantum optical metrology—the lowdown on high-n00n states,” *Contemporary physics*, vol. 49, no. 2, pp. 125–143, 2008.

[8] I. Afek, O. Ambar, and Y. Silberberg, “High-noon states by mixing quantum and classical light,” *Science*, vol. 328, no. 5980, pp. 879–881, 2010.

[9] J. F. Smith III, “Generation and detection of quantum entangled states for quantum imaging,” in *Quantum Information and Computation IX*, vol. 8057. SPIE, 2011, pp. 71–84.

[10] W.-B. Xing, X.-M. Hu, Y. Guo, B.-H. Liu, C.-F. Li, and G.-C. Guo, “Preparation of multiphoton high-dimensional ghz states,” *Optics Express*, vol. 31, no. 15, pp. 24 887–24 896, 2023.

[11] H.-Q. Liang, J.-M. Liu, S.-S. Feng, and J.-G. Chen, “Remote state preparation via a ghz-class state in noisy environments,” *Journal of Physics B: Atomic, Molecular and Optical Physics*, vol. 44, no. 11, p. 115506, 2011.

[12] Y. Ming, J. Tang, Z.-x. Chen, F. Xu, L.-j. Zhang, and Y.-q. Lu, “Generation of n00n state with orbital angular momentum in a twisted nonlinear photonic crystal,” *IEEE Journal of Selected Topics in Quantum Electronics*, vol. 21, no. 3, pp. 225–230, 2014.

[13] Y. Li, H. Jing, and M.-S. Zhan, “Optical generation of a hybrid entangled state via an entangling single-photon-added coherent state,” *Journal of Physics B: Atomic, Molecular and Optical Physics*, vol. 39, no. 9, p. 2107, 2006.

[14] C. F. Roos, M. Riebe, H. Haffner, W. Hansel, J. Benhelm, G. P. Lancaster, C. Becher, F. Schmidt-Kaler, and R. Blatt, “Control and measurement of three-qubit entangled states,” *science*, vol. 304, no. 5676, pp. 1478–1480, 2004.

[15] J. Joo, W. J. Munro, and T. P. Spiller, “Quantum metrology with entangled coherent states,” *Physical review letters*, vol. 107, no. 8, p. 083601, 2011.

[16] R. Demkowicz-Dobrzański, U. Dorner, B. Smith, J. Lundein, W. Wasilewski, K. Banaszek, and I. Walmsley, “Quantum phase estimation with lossy interferometers,” *Physical Review A*, vol. 80, no. 1, p. 013825, 2009.